Novel Fluorine-Bridged Polyfluorinated Iodine Structures. Presence of Fluorine as the Central Atom in a Five-Center, Six-Electron Bond

William B. Farnham,* David A. Dixon,* and Joseph C. Calabrese

Contribution No. 4113 from the Central Research and Development Department, E. I. du Pont de Nemours & Company, Inc., Experimental Station, Wilmington, Delaware 19898. *Received April 4, 1988*

Abstract: The reaction of tris(dialkylamino)sulfonium perfluoro-2-methyl-2-pentyl carbanion with perfluoro iodides (R_fI) leads to novel structures of the form $[R_f\text{–}I\text{–}F\text{–}I\text{–}R_f]^-$. The crystal structure for R_fI = pentafluorophenyl iodide reveals discrete ion pairs. The crystal structure for R_fI = 1,4-diiodooctafluorobutane shows an extended polymeric structure with $(CF_2)_4$ groups bridged by $[I\text{–}F\text{–}I]^-$ units. The I–F bond distances are 0.3–0.4 Å longer than normal fluorine–iodine distances but are >1.0 Å shorter than the sum of the van der Waals radii. The R_f–I–F bond angles are quasi-linear whereas the I–F–I bond angles deviate from linearity by 10°–20°. High-level ab initio calculations on $[F\text{–}I\text{–}F_c\text{–}I\text{–}F]^-$ and $[CF_3\text{–}I\text{–}F_c\text{–}I\text{–}CF_3]^-$ are presented. The free ions are calculated to have linear structures at I and at the central fluorine. The R_f–I bond distances are calculated to be slightly longer than those in a free R_f–I compound, and the I–F_c bond distances are significantly elongated as compared to free I–F. The vibrational analysis shows a very low bending frequency of 28 cm^{-1} at the central fluorine in $[F\text{–}I\text{–}F\text{–}I\text{–}F]^-$. Analysis of the wave functions shows that the bonding in these structures is best described by a five-center, six-electron (5c 6e) hypervalent σ bond and not as an ion–dipole complex. The 5c 6e bond is stabilized by more electronegative elements at the central and terminal positions and less electronegative elements at the other two positions. The negative charge is found at the central and terminal positions. The alkyl fluorides stabilize the excess negative charge at the terminal position by negative anionic hyperconjugation.

Atoms in unique bonding environments continue to be of great interest to chemists especially if the apparent bonding leads to violations of the Lewis octet rule. Although such atoms have often been described by sp^3d or sp^3d^2 hybridization,[1] there is little evidence for large amounts of d orbital character in the bonding of such molecules as PF_5, SF_4, ClF_3, and SF_6.[2,3] Rather, it is more appropriate to describe the electronic structure of such a molecule as being due to the presence of a three-center four-electron (3c 4e) bond, the hypervalent bond.[4,5] Recently, F as the central atom in such a hypervalent bond has been observed in argon matrices as F_3^-.[8] High-level ab initio calculations[5] on F_3^- show a symmetric $D_{\infty h}$ structure and support the 3c 4e model for the σ bonding.

It would be of great interest to isolate and structurally characterize any compound containing a first-row atom such as F as the central atom in a hypervalent 3c 4e bond. Previously, compounds containing boron[9] and carbon[10] as the central atom in such a bond have been reported but have not been isolated and subsequently structurally characterized. Our approach to the synthesis, isolation, and structural characterization of unusual anions is to prepare such anions with the tris(dialkylamino)sulfonium (TAS) cation.[11] This has allowed us to structurally characterize unusual species such as fluorosiliconates,[11b] perfluorinated alkoxides,[12] and perfluorinated carbanions.[13] As part of our examination of the chemistry of TAS perfluoro *tert*-butyl carbanion, we identified bis(perfluoro-*tert*-butyl)λ^3-iodanide as a stable TAS salt.[14] Structural variation of the carbanion and iodide reactants leads to different and unexpected products, and we report here the synthesis and characterization of an unprecedented class of fluorine-bridged iodine species **1** (eq 1). We report herein the crystal structures of an isolated anion **1** with R_f = pentafluorophenyl (**4**) and also the crystal structure of a polymeric species of **1** wherein $[I\text{–}F\text{–}I]^-$ units are bridged by the perfluoroalkyl group $-(CF_2)_4-$ (**5**).

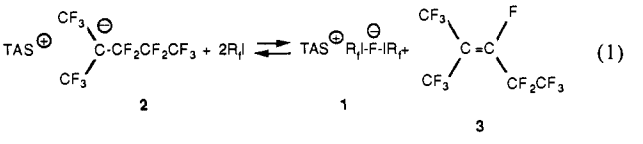

(1)

We have also found that the analysis of the structure and bonding of novel species is significantly aided if good ab initio calculations are available.[12,13c] We have thus performed high-quality ab initio, all-electron calculations on the model anions $[F\text{–}I\text{–}F\text{–}I\text{–}F]^-$ (**6**) and $[CF_3\text{–}I\text{–}F\text{–}I\text{–}CF_3]^-$ (**7**). Calculations on $[CF_3\text{–}I\text{–}CF_3]^-$ (**8**) were also done to test our ability to make structural predictions on a simple model system with iodine as the central atom in a hypervalent bond. Our results demonstrate that the central fluorine in **6** and **7** is in a hypervalent bonding situation if one allows for the extension of the 3c 4e bonding scheme to a 5c 6e bond for describing the σ bonds. Martin and Dykstra[5] define a hypervalent bonding species such as F_3^- as being a 3c 4e delocalized σ bond. This σ bond is the σ analogue (using p orbitals) of the familiar 3c 4e delocalized π bond of the allyl anion. Furthermore, the minimum energy structure of F_3^- in this model should be symmetric, i.e. have $D_{\infty h}$ symmetry. We can

(1) Huheey, J. E. *Inorganic Chemistry: Principles of Structure and Reactivity*; Harper and Row: New York, 1983.
(2) Keil, F.; Kutzelnigg, W. *J. Am. Chem. Soc.* **1975**, *97*, 3623.
(3) Hay, P. J. *J. Am. Chem. Soc.* **1977**, *99*, 1003.
(4) Musher, J. I. *Angew. Chem., Int. Ed. Engl.* **1969**, *8*, 54. Musher describes the hypervalent bond, the 3c 4e bond, in a valence bond description based on the models of Pimentel[6] and Rundle.[7]
(5) Cahill, P. A.; Dykstra, C. E.; Martin, J. C. *J. Am. Chem. Soc.* **1985**, *107*, 6359. These authors describe the hypervalent bond in simple molecular orbital terms following Musher's[4] valence bond description.
(6) Pimentel, G. C. *J. Chem. Phys.* **1951**, *19*, 446.
(7) Rundle, R. E. *Surv. Prog. Chem.* **1963**, *1*, 81.
(8) Ault, B. S.; Andrews, L. *J. Am. Chem. Soc.* **1976**, *98*, 1591; *Inorg. Chem.* **1977**, *16*, 2024.
(9) Lee, D. Y.; Martin, J. C. *J. Am. Chem. Soc.* **1984**, *106*, 5745.
(10) Forbus, T. R., Jr.; Martin, J. C. *J. Am. Chem. Soc.* **1979**, *101*, 5057.
(11) (a) Middleton, W. J. (to Du Pont) U.S. Patent 3,940,402, February 1976; *Org. Synth.* **1985**, *64*, 221. (b) Farnham, W. B.; Harlow, R. L. *J. Am. Chem. Soc.* **1981**, *103*, 4608.
(12) Farnham, W. B.; Smart, B. E.; Dixon, D. A.; Calabrese, J. C. *J. Am. Chem. Soc.* **1985**, *107*, 4565.
(13) (a) Smart, B. E.; Middleton, W. J.; Farnham, W. B. *J. Am. Chem. Soc.* **1986**, *108*, 4905. (b) Middleton, W. J. (to Du Pont) U.S. Patent 4,535,184. (c) Farnham, W. B.; Dixon, D. A.; Calabrese, J. C. *J. Am. Chem. Soc.* **1988**, *110*, 2607.
(14) $[(C_6F_5)_2I]^-$: Farnham, W. B.; Calabrese, J. C. *J. Am. Chem. Soc.* **1986**, *108*, 2449. We thank Dr. W. H. Powell (Chemical Abstracts Service) for bringing to our attention the preferred nomenclature for these new iodine species.

0002-7863/88/1510-8453$01.50/0 © 1988 American Chemical Society

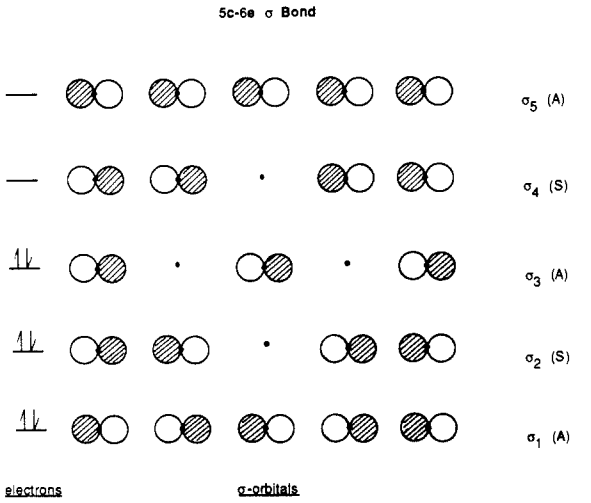

Figure 1. Simplified model for the 5c 6e hypervalent σ bond. The orbital coefficients are assumed to be equal. The S and A refer to symmetric and antisymmetric with regard to a plane perpendicular to the molecular axis and passing through the central atom. Note the nodal character of the orbitals. The energy increases from σ_1 to σ_5.

extend this definition to the 5c 6e σ bond by deriving the delocalized σ orbitals from the delocalized π orbitals of the pentadienyl anion. In Figure 1, we show a simple model based only on p_z orbitals for the delocalized σ orbital. (This model does not contain any s and d orbitals or account for differences in electronegativity.)

Experimental Section

General Remarks. Fluorine chemical shifts are reported in ppm from $CFCl_3$. Spectra were recorded on a Nicolet NT200 spectrometer at 188.2 MHz.

Some of the perfluoroalkyl iodides tend to become discolored upon standing. With the exception of the C_8 and C_{10} diiodides, which required only distillation, the distilled iodides used in this work were further purified immediately prior to use by vigorous shaking with excess mercury followed by transfer under vacuum of the liquid from mercury residues.

Solvents with minimum water concentration are required for preparation and manipulation of the complexes reported here. Tetrahydrofuran (THF), dimethoxyethane, and diethyl ether were distilled from sodium–benzophenone and then stored over activated molecular sieves. Acetonitrile and dimethylformamide (DMF) were distilled from calcium hydride and stored over activated sieves. All reactions were carried out in an atmosphere of dry nitrogen, and manipulations of the complexes were performed in a Vacuum Atmospheres drybox.

Synthesis. Fluoride Adduct of Pentafluorophenyl Iodide (4). A solution of TAS 1,1,1,3,3,4,4,5,5,5-decafluoro-2-(trifluoromethyl)-2-pentanide[3] (**2**; 4.84 g, 10 mmol) in THF (20 mL) was treated with pentafluorophenyl iodide (6.0 g, 20 mmol), and the resulting solution was stirred at ambient temperature for 1.0 h. Removal of volatiles under reduced pressure provided 7.5 g of white solid, which was crystallized from THF/ether to give 6.65 g (86%); mp 140–141 °C. ^{19}F NMR (THF-d_8): −53.0 (s, 1 F), −120.85 (m, 4 F), −158.43 (t, J = 20 Hz, 2 F), −162.89 (m, 4 F). Anal. C, H, N, F, I.

Fluoride Adduct of 1,4-Diiodooctafluorobutane (5). A solution of TAS carbanion **2** (4.84 g, 10 mmol) in THF (30 mL) was treated with 1,4-diiodooctafluorobutane (4.54 g, 10 mmol), and the resulting solution was stirred for 0.5 h. Evaporation gave a residue, which was triturated twice with THF and recrystallized from methylene chloride/*tert*-butyl methyl ether to provide 5.5 g (86%) of colorless crystals, mp 132 °C (dec). ^{19}F NMR (CD_2Cl_2): −74.05 (s, 1 F), −75.61 (m, 4 F), −112.95 (m, 4 F). Anal. C, H, F, N, S, I.

Fluoride Adduct of Perfluoro-*n*-hexyl Iodide (9). A solution of TAS carbanion **2** (9.68 g, 20 mmol) in THF (35 mL) was treated with perfluoro-*n*-hexyl iodide (17.8 g, 40 mmol), and the resulting solution was stirred for 0.5 h. Volatiles were removed under vacuum to give a residue, which was recrystallized from *tert*-butyl methyl ether at ca. −20 °C to provide 16.3 g (76%) of colorless crystals, mp 62–63 °C. ^{19}F NMR (THF-d_8): −75.3 (br s, 1 F), −77.35 (m, 4 F), −80.76 (m, 6 F), −114.43 (m, 4 F), −120.83 (m, 4 F), −122.50 (m, 4 F), −125.94 (m, 4 F). Anal. C, H, F, N, S, I.

Fluoride Adduct of 1,2-Diiodotetrafluoroethane (10). A solution of TAS carbanion **2** (4.84 g, 10 mmol) in THF (25 mL) was treated with 1,2-diiodotetrafluoroethane (3.54 g, 10 mmol), and the resulting solution was stirred for 0.5 h. Evaporation gave 5.5 g of crude residue, which was triturated with *tert*-butyl methyl ether/THF and filtered to give 3.81 g of colorless solid, mp 98–99 °C (dec). ^{19}F NMR (CD_2Cl_2): −60.94 (br s, 4 F), −80.5 (br s, 1 F).

Fluoride Adduct of 1,8-Diiodohexadecafluorooctane (11). The adduct **11** was prepared as described for **5** with TAS carbanion **2** (2.42 g, 5.0 mmol) and 1,8-diiodohexadecafluorooctane (3.27 g, 5.0 mmol). Trituration of the solid with THF gave 2.65 g; mp 77–78 °C (dec). ^{19}F NMR (CD_2Cl_2): −74.55 (m, 4 F), −82.0 (s, 1 F), −115.0 (m, 4 F), −121.0 and −122.0 (m, 8 F). Anal. C, H, N, F, I.

Fluoride Adduct of 1,10-Diiodoeicosafluorodecane (12). The adduct **12** was prepared as described for **5** with TAS carbanion **2** (2.42 g, 5.0 mmol) and 1,10-diiodoeicosafluorodecane (3.77 g, 5.0 mmol). The crude product was taken up in THF (ca. 25 mL), cooled to −20 °C, and filtered to give 3.95 g; mp 114–115 °C (dec). ^{19}F NMR (DMF-d_7): −73.10 (br s, 1 F), −74.0 (t, J = 14 Hz, 4 F), −114.05 (br s, 4 F), −120.17 (br s, 4 F), −121.06 (br s, 8 F). Anal. C, H, N, F, I.

Crystal Structure Analysis. Crystal Growth. Crystals of **4** were grown by slow diffusion of methyl *tert*-butyl ether into a THF solution of **4**. Crystals of **5** were obtained by slow diffusion of methyl *tert*-butyl ether into a CH_2Cl_2/THF solution of **5**.

Crystal data for 4: $C_{18}H_{18}N_3F_{11}I_2S$, monoclinic; space group $P2_1/C$ (No. 14); a = 12.440 (1), b = 19.279 (3), c = 10.700 (2) Å; β = 102.08 (1)°; V = 2509.4 Å^3; Z = 4; T = −100 °C. A Syntex R3 diffractometer equipped with a graphite monochromator, λ(Mo Kα) = 0.71069 Å, was used to obtain cell and intensity data out to 2θ = 55°. The ω scan method was used, with scan width 1.00°ω and scan speed 2.00–9.80°/min for 4.2° < 2θ < 55.0°. Typical half-height peak width = 0.25°ω. Three standards were monitored at regular intervals, and data were corrected for a 13% decrease in intensity. Out of 6253 independent reflections, 3519 were considered to be observed at the 3.0$\sigma(I)$ significance level. Data were corrected for absorption (DIFABS) and for a 23.8% variation in azimuthal scan.

Solution and Refinement of Structure 4. The structure was solved by automated Patterson analysis (PHASE) with full-matrix, least-squares refinement. Scattering factors were from ref 15, including anomalous terms for I and S. All hydrogens were refined isotropically, and other atoms, anisotropically. The final agreement factors were R = 0.041 and R_w = 0.042 for 316 independent variables.

Crystal data for 5: $C_{14}H_{26}F_9N_3I_2SO$, orthorhombic; space group *Pnma* (No. 62); a = 24.764 (3), b = 9.872 (1), c = 9.960 (1) Å; V = 2459.6 Å^3; Z = 4; T = −100 °C. A Syntex R3 diffractometer equipped with a graphite monochromator, λ(Mo Kα) = 0.71069 Å, was used to obtain cell and intensity data out to 2θ = 55°. The ω scan method was used, with scan width 1.20°ω and scan speed = 3.90–9.80°/min for 4.1° < 2θ < 55.0°. Typical half-height peak width = 0.29°ω. Three standards were monitored at regular intervals, and data were corrected for a 9% decrease in intensity. Out of 3239 independent reflections, 2245 were considered to be observed at the 3.0$\sigma(I)$ significance level. Data were corrected for absorption (DIFABS) and for a 16.2% variation in azimuthal scan.

Solution and Refinement of Structure 5. The structure was solved by automated Patterson analysis (PHASE) using full-matrix, least-squares refinement. Scattering factors were from ref 15, including anomalous terms for I and S. All hydrogens were refined isotropically, and other atoms, anisotropically. The final agreement factors were R = 0.030 and R_w = 0.034 for 157 independent variables. The solution was made difficult by the predominance of atoms lying on mirror planes. All three units of the structure, the R–I–F–I–R chain, TAS, and THF, lie on mirror planes. The thermal parameters of the THF molecule indicate disorder away from the mirror plane. It is assumed that this would not provide enough scattering power to warrant a lower space group symmetry.

Calculations. Ab initio molecular orbital calculations involving all electrons were performed on **6–8**. Geometries were gradient optimized[16] with the program HONDO[17] on an IBM-3081. Calculations on $[F–I–F–I–F]^-$ (**6**) were done in $D_{\infty h}$ symmetry and the calculations on $[CF_3–I–F–I–CF_3]^-$ (**7**) and $[CF_3–I–CF_3]^-$ (**8**) in D_{3h} symmetry. The fluorine basis set for **6** is of polarized double-ζ quality with coefficients from Dunning and Hay.[18] The basis set for the central fluorine, F_c, was

(15) *International Tables for X-ray Crystallography*; Kynoch: Birmingham, England, 1974; Vol. IV.

(16) (a) Komornicki, A.; Ishida, K.; Morokuma, K.; Ditchfield, R.; Conrad, M. *Chem. Phys. Lett.* **1977**, *45*, 595. McIver, J. W., Jr.; Komornicki, A. *Ibid.* **1971**, *10*, 303. (b) Pulay, P. In *Applications of Electronic Structure Theory*; Schaefer, H. F., III, Ed.; Plenum: New York, 1977; p 153.

(17) (a) Dupuis, M.; Rys, J.; King, H. F. *J. Chem. Phys.* **1976**, *65*, 111. (b) King, H. F.; Dupuis, M.; Rys, J. *National Resource for Computer Chemistry Software Catalog*, Program QHO2 (HONDO), 1980; Vol. 1.

Table I. Physical Properties of Anions with F as the Central Atom in a 5c 6e Bond[a]

anion structure	mp,[b] °C	λ, nm (ϵ,[c] M^{-1} cm^{-1})	λ, nm (ϵ,[d] M^{-1} cm^{-1})
C_6F_5I–F–IC_6F_5 (**4**)	140–141	251 (5900) 226 (27800)	260 (sh) (2300)
(n-C_6F_{13})I–F–I(n-C_6F_{13}) (**9**)	62–63	252 (11700)	275 (sh) (605)
$[I(CF_2)_2I–F]_n$ (**10**)	98–99		
$[I(CF_2)_4I–F]_n$ (**5**)	132		273 (sh) (660)
$[I(CF_2)_8I–F]_n$ (**11**)	77–78		
$[I(CF_2)_{10}I–F]_n$ (**12**)	114–115		

[a] Cation in all examples is tris(dimethylamino)sulfonium. [b] Satisfactory elemental analyses (C, H, N, S, F, I) were obtained for all new compounds. [c] THF solution. [d] CH_2Cl_2 solution.

augmented with a set of diffuse s ($\alpha_s = 0.096$) and p functions[18] on the possibility that it was simply a bridging fluoride anion. The iodine basis set is from Huzinaga and co-workers[19] and is a split-valence basis set augmented by a set of valence d polarization functions ($\alpha_d = 0.266$). The final basis set for **6** has the form (16s13p8d/10s6p1d/9s5p1d)/[6s5p3d/4s3p1d/3s2p1d] in the order $I/F_c/F_T$. For **7**, the I and F_c basis sets were the same as those in **6**. The basis set for the C and F in the CF_3 groups is the Dunning and Hay[18] s and p basis set given above, (9s5p)/[3s2p]. This will give terminal C–F bond distances that are somewhat long. The basis set for **8** is the I basis set given above for **6** together with the CF_3 basis set given for **7**. The total number of contracted basis functions is 127 for **6**, 169 for **7**, and 111 for **8**. For **6** and **8**, the force field was determined with analytic second derivatives, and infrared intensities were also calculated.[20] These calculations were done with the program GRADSCF[21] on a CRAY-1A computer.

Results

Chemistry and Spectroscopy. One reaction exhibited by stable TAS perfluoro carbanion salts[3] is fluoride transfer to an acceptor that has a higher fluoride affinity than the precursor perfluoroolefin. In some cases, the reaction may be driven contrathermodynamically by physical removal of the perfluoroolefin. Thus, although treatment of perfluoro carbanion salt **2** with a perfluoroalkyl or perfluoroaryl iodide results in no spectroscopically observable reaction, removal of fluoroolefin **3** leads to high yields of adduct **1** (eq 1). A variety of fluorinated iodides are applicable in this process (Table I), but nonfluorinated iodides (e.g. C_6H_5I) do not yield stable adducts. Apparently, fluorine substitution in the anion of **1** is required for stabilization presumably due to negative anionic hyperconjugation.[12,13] Use of α,ω-perfluoro diiodides leads to infinite chain structures such as **5** and **10–12**.

Electronic absorption spectra of the complexes are solvent dependent and exhibit enhanced extinction coefficients in tetrahydrofuran (but not in dichloromethane) by comparison with the neutral R_fI precursors (see Table I). Complexes **5** and **10–12** are not sufficiently soluble in solvents in which the enhanced ϵ of **9** is observable.

The ^{19}F chemical shift of the unique, bridging fluorine in complexes **4**, **5**, and **9–12** is dependent upon the identity of R_f bound to I, but not in a predictable fashion. The shifts, which are moderately solvent dependent and are at a substantially lower field than other reported fluorides,[22] may result from the unusual coordination number in the I–F–I complexes.

We attempted to assess the magnitude of the I–F bond energy in complexes **4** and **9** by examining the degenerate exchange of free R_fI with the anionic complex. Even at low temperature, only exchange-averaged signals are observed by ^{19}F NMR (in THF or CD_2Cl_2) in such solutions with **4** and **5**.

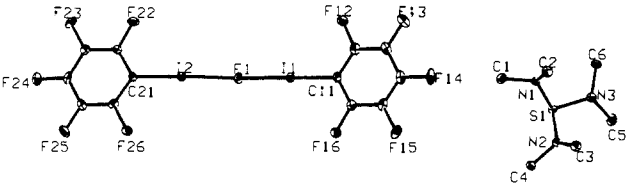

Figure 2. Molecular drawing of **4** based on the crystal structure data.

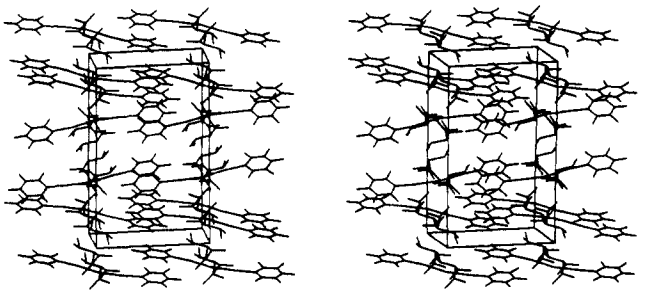

Figure 3. Packing diagram for **4**.

Table II. Bond Distances and Angles for **4**[a] from the X-ray Structure

	Interatomic Distances (Å)		
I1–F1	2.455 (4)	N1–C2	1.482 (10)
I2–F1	2.509 (4)	N2–C3	1.463 (9)
I1–C11	2.130 (7)	N2–C4	1.462 (9)
I2–C21	2.096 (7)	N3–C5	1.465 (10)
S1–N1	1.619 (6)	N3–C6	1.494 (9)
S1–N2	1.622 (6)	C11–C12	1.379 (11)
S1–N3	1.682 (6)	C11–C16	1.400 (10)
F12–C12	1.346 (9)	C12–C13	1.369 (11)
F13–C13	1.360 (9)	C13–C14	1.393 (12)
F14–C14	1.340 (9)	C14–C15	1.357 (12)
F15–C15	1.352 (9)	C15–C16	1.380 (10)
F16–C16	1.320 (9)	C21–C22	1.383 (10)
F22–C22	1.344 (8)	C21–C26	1.400 (10)
F23–C23	1.338 (8)	C22–C23	1.391 (10)
F24–C24	1.335 (8)	C23–C24	1.384 (11)
F25–C25	1.349 (9)	C24–C25	1.370 (11)
F26–C26	1.348 (8)	C25–C26	1.375 (10)
N1–C1	1.458 (9)		
	Intramolecular Angles (deg)		
F1–I1–C11	175.6 (3)	F15–C15–C16	119.0 (8)
F1–I2–C21	176.8 (3)	F16–C16–C11	120.5 (7)
N1–S1–N2	115.6 (3)	F16–C16–C15	119.4 (7)
N1–S1–N3	100.8 (3)	F22–C22–C21	120.4 (6)
N2–S1–N3	98.5 (3)	F22–C22–C23	117.0 (7)
I1–F1–I2	169.0 (2)	F23–C23–C22	121.1 (7)
S1–N1–C1	114.0 (5)	F23–C23–C24	119.8 (7)
S1–N1–C2	121.4 (5)	F24–C24–C23	120.3 (7)
S1–N2–C3	125.1 (5)	F24–C24–C25	119.6 (8)
S1–N2–C4	114.5 (5)	F25–C25–C24	120.0 (7)
S1–N3–C5	110.9 (5)	F25–C25–C26	120.1 (7)
S1–N3–C6	113.8 (5)	F26–C26–C21	119.0 (7)
C1–N1–C2	114.6 (6)	F26–C26–C25	118.5 (7)
C3–N2–C4	115.5 (6)	C12–C11–C16	117.3 (7)
C5–N3–C6	110.6 (6)	C11–C12–C13	122.3 (8)
I1–C11–C12	120.9 (6)	C12–C13–C14	119.7 (8)
I1–C11–C16	121.6 (6)	C13–C14–C15	118.8 (8)
I2–C21–C22	122.4 (5)	C14–C15–C16	121.7 (8)
I2–C21–C26	121.6 (5)	C11–C16–C15	120.2 (7)
F12–C12–C11	120.4 (7)	C22–C21–C26	116.0 (6)
F12–C12–C13	117.3 (8)	C21–C22–C23	122.6 (7)
F13–C13–C12	121.1 (8)	C22–C23–C24	119.0 (7)
F13–C13–C14	119.2 (7)	C23–C24–C25	120.1 (7)
F14–C14–C13	119.5 (8)	C24–C25–C26	119.8 (7)
F14–C14–C15	121.7 (8)	C21–C26–C25	122.5 (7)
F15–C15–C14	119.3 (7)		

[a] See Figure 2 for numbering scheme.

Studies of the reactivity of adducts **1** indicate that they serve as sources of loosely bound fluoride ion in solution. For example, the adduct **4** converts fluoroolefin **3** to the carbanion **2**, benzyl bromide to benzyl fluoride, and *O*-(trimethylsilyl)phenol to 4-

(18) Dunning, T. H., Jr.; Hay, P. J. In *Methods of Electronic Structure Theory*; Schaefer, H. F., III, Ed.; Plenum: New York, 1977; p 1.
(19) *Gaussian Basis Sets for Molecular Calculations*; Huzinaga, S., Ed.; Physical Sciences Data 16; Elsevier: Amsterdam, The Netherlands, 1984.
(20) King, H. F.; Komornicki, A. In *Geometrical Derivatives of Energy Surfaces and Molecular Properties*; Jorgenson, P., Simons, J., Ed.; NATO ASI Series C; Reidel: Dordrecht, The Netherlands, 1986; p 207. King, H. F.; Komornicki, A. *J. Chem. Phys.* **1986**, *84*, 5645.
(21) GRADSCF is an ab initio gradient program system designed and written by A. Komornicki at Polyatomics Research.
(22) See: Clark, J. H.; Goodman, E. M.; Smith, D. K.; Brown, S. J.; Miller, J. M. *J. Chem. Soc., Chem. Commun.* **1986**, 657.

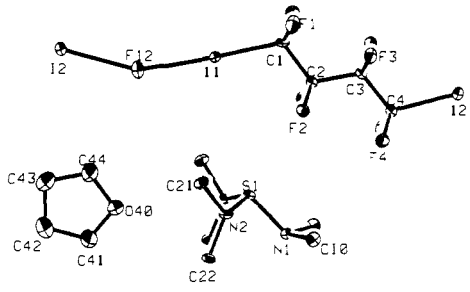

Figure 4. Molecular drawing of the unique fragment in **5** based on the crystal structure data. The compound crystallizes with one THF solvent molecule per I–F–I fragment.

Table III. Unique Bond Distances and Angles for **5**[a] from the X-ray Structure

	Interatomic Distances (Å)		
I1–F12	2.438 (3)	O40–C44	1.360 (11)
I2–F12	2.466 (4)	N1–C10	1.473 (5)
I1–C1	2.152 (6)	N2–C21	1.473 (5)
I2–C4a[b]	2.162 (6)	N2–C22	1.476 (4)
S1—N1	1.681 (5)	C1–C2	1.554 (8)
S1–N2	1.618 (3)	C2–C3	1.560 (8)
F1–C1	1.357 (4)	C3–C4	1.539 (8)
F2–C2	1.342 (4)	C41–C42	1.418 (15)
F3–C3	1.345 (4)	C42–C43	1.447 (16)
F4–C4	1.353 (4)	C43–C44	1.389 (14)
O40–C41	1.283 (11)		
	Intramolecular Angles (deg)		
F12–I1–C1	177.1 (2)	F2–C2–F2b[b]	108.8 (4)
F12–I2–C4a[b]	180 (4)	F3–C3–F3b[b]	107.7 (5)
N1–S1–N2	99.2 (1)	F4–C4–F4b[b]	106.8 (5)
N2–S1–N2b[b]	117.7 (3)	F1–C1–C2	107.8 (4)
I1–F12–I2	155.8 (2)	F2–C2–C1	107.8 (3)
C41–O40–C44	103.9 (8)	F2–C2–C3	108.1 (3)
S1–N1–C10	112.2 (3)	F3–C3–C2	108.0 (3)
S1–N2–C21	115.1 (3)	F3–C3–C4	107.8 (3)
S1–N2–C22	123.0 (3)	F4–C4–C3	108.4 (3)
C10–N1–C10b[b]	110.7 (5)	O40–C41–C42	116 (1)
C21–N2–C22	115.0 (3)	O40–C44–C43	114 (1)
I1–C1–F1	110.3 (3)	C1–C2–C3	116.1 (5)
12c–C4–F4[b]	110.2 (3)	C2–C3–C4	117.1 (5)
I1–C1–C2	114.5 (4)	C41–C42–C43	102 (1)
12c–C4–C3[b]	112.6 (4)	C42–C43–C44	104 (1)
F1–C1–F1b[b]	105.8 (5)		

[a] See Figure 4 for numbering. [b] a, $^1/_2 + x, y, {}^3/_2 - z$; b, $x, {}^1/_2 - y, z$; c, $^1/_2 + x, y, {}^3/_2 - z$.

phenoxy-2,3,5,6-tetrafluoro-1-iodobenzene.[23] Treatment of the adducts with water affords the corresponding free fluorocarbon iodides.

Crystal Structures. Single-crystal X-ray diffraction analysis of the pentafluorophenyl adduct **4** (Figure 2) reveals a nearly linear I–F–I array (θ(I–F–I) = 169°) with rather long I–F distances (2.509 (4), 2.455 (4) Å) (see Table II for bond distances and angles). Carbon–iodine bond distances (2.130, 2.096 Å) are only slightly elongated by comparison with that in 1,4-diiodotetrafluorobenzene (2.089 Å)[24] and are substantially shorter than those determined for bis(pentafluorophenyl)λ^3-iodanide (2.331, 2.403 Å).[14] Bond lengths and angles within the aromatic rings appear to be normal. Each anion is surrounded in the crystal by four TAS cations (Figure 3). The geometrical features of the TAS cation are similar to those of other TAS salts.[11b,12,25] The cations appear to interact most strongly with the fluorine in the I–F–I unit. The largest concentration of negative charge (see below) is expected at this fluorine.

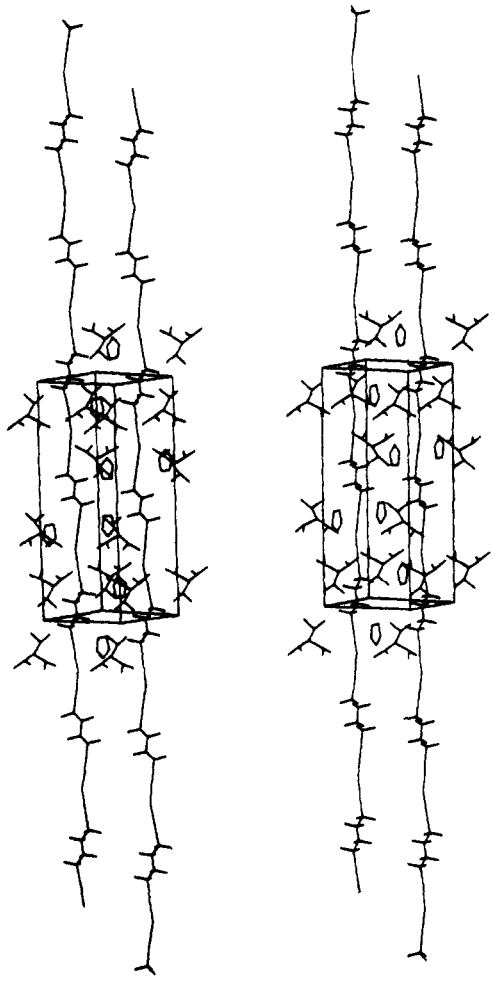

Figure 5. Packing diagram for **5**.

Single-crystal X-ray diffraction analysis of **5** shows that the anionic portion consists of infinite chains of alternating C_4F_8 and I–F–I fragments (Figure 4). The conformation of the C_4F_8 segment is of note since a perfectly staggered arrangement is realized.[26] The I–F–I angles are somewhat more acute than in the case of **4**, and the fluorine–iodine distances are slightly shorter (see Table III for bond distances and angles). The C–F bonds in the CF_2 groups bonded to the iodine are 0.01 Å longer than the C–F bonds on the interior CF_2 groups (bonded to two carbons). The values for θ(F–C–F) on the CF_2 groups bonded to iodine are 2° smaller than those at the interior CF_2 groups. This indicates that the CF_2 groups bonded to iodine have more negative charge than do the interior CF_2 groups. The packing arrangement in **7** features separated polyanionic chains and TAS cations along with one THF molecule per I–F–I fragment (Figure 5). The TAS cations interact most strongly with the central fluorine in the I–F–I moiety and with the CF_2 group bonded to I. This is where the negative charge is expected to be concentrated (see below). The THF molecules interact with the TAS cations and with the iodines in the chain, which should have excess positive charge.

Calculations. In order to test our basis sets and techniques, calculations were first done on CF_3I with the basis set used for

(23) Nucleophilic displacement of fluoride from halopentafluorobenzene normally occurs at the para position. See: Kobrina, L. S. *Fluorine Chemistry Reviews*; Tarrant, P., Ed.; Dekker: New York, 1976; Vol. 7.

(24) Few C–I distances have been determined for polyfluorinated aromatic systems. We regard 1,4-diiodotetrafluorobenzene as representative of this class. Chaplot, S. L.; McIntyre, G. J.; Mierzejewski, A.; Pawley, G. S. *Acta Crystallogr., Sect. B* **1981**, *37*, 2210.

(25) Farnham, W. B.; Dixon, D. A.; Middleton, W. J.; Calabrese, J. C.; Harlow, R. L.; Whitney, J. F.; Jones, G. A.; Guggenberger, L. J. *J. Am. Chem. Soc.* **1987**, *109*, 476.

(26) Although Teflon has a helical structure (Phase II and IV), some short chain (n = 4,6) examples have been interpreted as existing in the all-trans form: Bunn, C. W.; Howells, E. R. *Nature (London)* **1954**, *174*, 549. Campos-Vallette, M.; Rey-Lafon, M. *J. Mol. Struct.* **1983**, *101*, 23. Bates, T. W. In *Fluoropolymers*; Wall, L. A., Ed.; Wiley-Interscience: New York, 1972; Chapter 13, pp 451–474. Campos-Vallette, M.; Rey-Lafon, M. *J. Mol. Struct.* **1984**, *118*, 245. However, ab initio calculations indicate an energy difference of 0.5 kcal/mol for the C_2 helical and C_{2h} trans conformations of perfluoro-*n*-butane. Dixon, D. A.; Van-Catledge, F. A. *Int. J. Supercomputer Applications* **1988**, 2(No. 2), 62.

Table IV. Calculated Molecular Parameters for IF and CF_3I[a]

param	calc	expt[b]
	I–F	
r(I–F)	1.917	1.910
ω_e[d]	677	610
	CF_3I (Structure)[c]	
r(C–F)	1.366	1.344 (4)
r(C–I)	2.133	2.101 (9)
θ(F–C–F)	107.0	107.6
θ(F–C–I)	111.9	111.3

CF_3I (Frequencies)

sym	ν_{calc}[d]	scale[e]	I_{calc}[f]	ν_{expt}[d,g]	I_{expt}[f,g]
a_1	1154	0.93	516.3	1074	573.3 ± 16.9
	732	1.02	31.2	743	43.0 ± 1.4
	315	0.90	6.2	284	0.15 ± 0.03
e	1220	0.97	494.5	1185	445.2 ± 29.2
	524	1.03	10.9	539	2.1 ± 0.3
	277	0.94	0.2	260	0.04 ± 0.01

[a] Bond distances in angstroms. Bond angles in degrees. [b] Reference 27. [c] Reference 28. [d] Frequency in reciprocal centimeters. [e] Scale factor = ν_{expt}/ν_{calc}. [f] Infrared intensity in kilometers per mole. [g] Reference 30.

7 and on IF with the I/F basis set used for **6**. The results are shown in Table IV where they are compared to experiment.[27,28] The calculated bond length of 1.917 Å in IF is in excellent agreement with the experimental distance of 1.910 Å.[27] The calculated stretching frequency in IF is too high as expected, 677 cm^{-1} (I = 59 km/mol), calculated vs 610 cm^{-1}, experimental.[27]

The calculated structure for CF_3I is in good agreement with the experimental one[28] although the agreement is not as good as found for IF. The calculated C–F and C–I bond lengths are too large by 0.02 and 0.03 Å, respectively, a result expected because of our neglect of polarization functions on the carbon.[29] The calculated angles show excellent agreement with experiment and are within 0.6°. The calculated frequencies are in reasonable agreement with experiment.[30] The C–F and C–I stretches are larger than the experimental values, as is the bend involving the iodine. The frequencies for the CF_3 deformations are calculated to be too low by 2–3%. The calculated intensities are also in reasonable agreement with the experimental values. The calculated intensities for the very intense C–F stretches show very good agreement as does the calculated intensity of the CF_3 deformation of a_1 symmetry. The remaining intensities are small and are calculated to be somewhat larger than the experimental values. The correct ordering of the intensities is given by theory. The above results show quite good overall agreement between theory and experiment even though the CF_3 group is treated with only a double-ζ basis set.

Since our basis set is adequate for treating the monomeric CF_3I and IF units, we calculated the structure of **8** in order to demonstrate that iodine in a hypervalent bond can also be described before studying **6** and **7**. The calculated structure for $[CF_3–I–CF_3]^-$, is given in Table V. We can compare these values to r(C–I) = 2.367 and θ(C–I–C) = 175.2 from the crystal structure of $[C_6F_5–I–C_6F_5]^-$. (The value of 2.367 Å is obtained by averaging the two values for r(C–I) of 2.403 and 2.331 Å.) The calculated D_{3h} structure for **8** is a minimum as determined by a force field calculation (see below). The calculated values for r(C–I) and θ(C–I–C) are in excellent agreement with the experimental values considering that our calculation is for the isolated gas-phase ion and the experimental structure is from the crystal with cations

Table V. Calculated Molecular Parameters for **8**

Structure[a]

param	calc	param	calc
r(C–I)	2.352	θ(C–I–C)	180.0
r(C–F)	1.404	θ(F–C–F)	103.4
		θ(F–C–I)	115.0

Frequencies

sym	ν_{calc}[b]	I[c]
a_1'	1169	0
	685	0
	189	0
e′	1085	1163
	509	2
	264	4
	68	8
a_1''	9	0
a_2''	1160	532
	673	0
	131	192
e″	1069	0
	496	0
	179	0

[a] Bond distances in angstroms. Bond angles in degrees. [b] Frequency in reciprocal centimeters. [c] Infrared intensity in kilometers per mole.

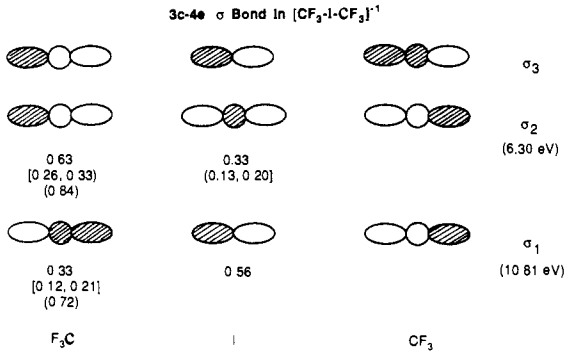

Figure 6. Schematic of the 3c 4e hypervalent σ bond in **8**. The energies and populations are given for the occupied orbitals. The populations directly beneath the orbital are the total atomic charge in that orbital in units of electrons. The populations in brackets are the s and p components on C and the s and d components on I. The population in parentheses is the CF_3 group population. Orbitals with two lobes of the same phase are d functions.

present. The difference in θ(C–I–C) is consistent with the presence of a very low frequency for bending (see below). The C–I bond has elongated by 0.22 Å in **8** as compared to the calculated value in CF_3I consistent with formation of a 3c 4e bond. The CF_3 groups are clearly different from that in CF_3I. The C–F bond in **8** is elongated by 0.04 Å and θ(F–C–F) is decreased by 3.6° as compared to CF_3I. These changes are similar to those calculated in other carbanions and are consistent with a significant transfer of negative charge to the CF_3 groups due to negative anionic hyperconjugation.[12,13,29]

The vibrational frequencies for **8** are shown in Table V. The results clearly show that the D_{3h} structure is a minimum although the torsion frequency is only 9 cm^{-1}. The six highest energy modes are assigned to CF stretches and the allowed stretches are predicted to be intense. The frequencies 685 (a_1'), 509 (e′), 673 (a_2'') and 496 (e″) cm^{-1} can be assigned to CF_3 deformations. The frequencies at 264 (e′) and 179 (e″) cm^{-1} are assigned to CF_3 rocks. The symmetric C–I–C stretch is at 189 (a_1') cm^{-1} whereas the asymmetric C–I–C stretch is at 131 (a_2'') cm^{-1}. The e′ band at 68 cm^{-1} is the C–I–C bend. The small value for this bend is consistent with the slight deviation from linearity found for [C6F5–I–C6F5]$^-$ in the crystal. It is clear from our calculations that we can treat iodine in the 3c 4e hypervalent bond.

The atomic charges are consistent with the model of the 3c 4e bond expected for **8**. The iodine is positive (+0.20e) and the CF_3 groups are negative (–0.60e) with a charge on C of +0.52e and

(27) Huber, K. P.; Herzberg, G. *Constants of Diatomic Molecules*; Van Nostrand Reinhold: New York, 1979.
(28) Andreassen, A. L.; Bauer, S. H. *J. Chem. Phys.* **1972**, *56*, 3802.
(29) Dixon, D. A.; Fukunaga, T.; Smart, B. E. *J. Am. Chem. Soc.* **1986**, *108*, 1585, 4027. Dixon, D. A. *J. Phys. Chem.* **1986**, *90*, 2038.
(30) (a) Smith, M. A. H.; Rinsland, C. P.; Fridovich, B.; Rao, K. N. In *Molecular Spectroscopy: Modern Research*; Rao, K. N., Ed.; Academic: New York, 1985; Vol. III, p 111. (b) Person, W. B.; Rudys, S. K.; Newton, J. K. *J. Phys. Chem.* **1975**, *79*, 2525.

Table VI. Calculated Molecular Parameters for **6**

Geometry[a]		
param	calc	$Xe_2F_3^{+}$ [b]
$r(I-F_T)$	1.993	1.90 ± 0.03
$r(I-F_c)$	2.278	2.14 ± 0.03
$\theta(F_T-I-F_c)$	180.0	178 ± 2
$\theta(I-F_c-I)$	180.0	151 ± 2

Spectrum		
sym	ν_{calc}[c]	I_{calc}[d]
σ_g^+	578	0
	114	0
π_g	152	0
σ_u^+	573	185
	329	858
π_u	217	58
	28	2

[a] Bond distances in angstroms. Bond angles in degrees. [b] Reference 33. [c] Frequency in reciprocal centimeters. [d] Infrared intensity in kilometers per mole.

a charge on F of −0.37e. The high negative charge on F is consistent with fluorine negative anionic hyperconjugation.

The HOMO for **8** is a σ orbital (IP = 6.30 eV) with the largest density on the CF_3 groups (see Figure 6). The central atom has a population of 0.33e in s and $3d_{z^2}$ orbitals. The carbons have 0.63e each, with the remaining charge on the fluorines. The orbital is symmetric, and the s orbitals on the C's and on I are separated by nodal planes; the p_z orbitals on the C are also antibonding with respect to the s on iodine. However, there is a bonding interaction between the d_{z^2} on I and the p_z orbitals on the carbons. The NHOMO (7.02 eV) is a degenerate orbital, the iodine lone pairs. The next orbital is the bonding σ orbital component (10.81 eV) of the 3c 4e bond. Here, the largest population is in the p_z orbital on iodine (0.56e), and there are populations of 0.33e on the carbons in s and p orbitals. There is some delocalization to the fluorines with each fluorine contributing 0.13e. Thus, each CF_3 group has 0.72e on it, more than on the central atom. This is consistent with the lower electronegativity of I and the ability of the fluorines to stabilize excess negative charge on the CF_3 groups by negative anionic hyperconjugation. The LUMO is the expected antibonding σ orbital with the largest coefficients due to the p_z on the iodine followed by the s coefficients on the carbon.

The calculated structure for the model compound **6** is given in Table VI together with the vibrational analysis. The molecule has $D_{\infty h}$ symmetry as shown by the vibrational analysis. The $I-F_T$ bonds are elongated by 0.076 Å as compared to the I–F diatomic bond whereas the $I-F_c$ bond is much longer, 0.36 Å, than the diatomic bond. This elongation is significantly larger than the elongation seen when the C–I bonds in **8** and CF_3I are compared.

The highest energy vibrational band at 578 cm^{-1} (σ_g^+) is the symmetric $I-F_T$ stretch, and the σ_u^+ band at 573 cm^{-1} is the asymmetric $I-F_T$ stretch. These values are ~100 cm^{-1} lower than the calculated stretching frequency in diatomic IF consistent with the increase of the $I-F_T$ bond length in **6**. The very intense σ_u^+ band at 329 cm^{-1} is the asymmetric $I-F_c-I$ stretch and the symmetric $I-F_c-I$, σ_g^+ stretch is much lower at 114 cm^{-1}. The real value for the asymmetric stretch shows that **6** is stable at the SCF level with respect to dissociation to IF and $[FIF]^-$. This differs from F_3^- where F_3^- is unstable with respect to dissociation to F^- and F_2 at the SCF level.[5] The π_g bend at 156 cm^{-1} does not involve motion at the F_c and is predominantly a wag of the terminal fluorines. The two π_u bends both involve motion of the central fluorine. The π_u bend at 217 cm^{-1} has a significant iodine component whereas the low-frequency π_u bend at 28 cm^{-1} has only a small component of bending at the iodines. The very low frequency bend of 28 cm^{-1} shows that these molecules are very floppy. This suggests that significant deviations from linearity in the crystal for $[R_f-I-F-I-R_f]^-$ would not be surprising and that the deviation would occur by bending at F_c. As discussed above, the TAS cations interact with F_c in the crystal structure of both **4** and **5** and crystal-packing forces could easily lead to the observed distortions from linearity at F_c.

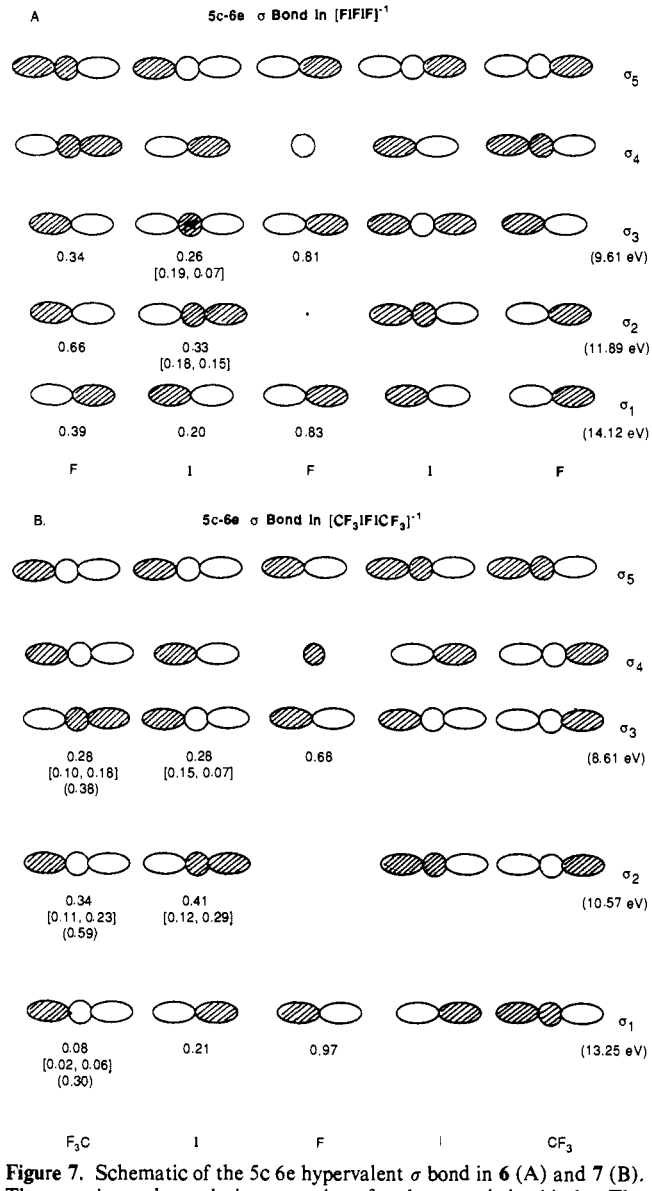

Figure 7. Schematic of the 5c 6e hypervalent σ bond in **6** (A) and **7** (B). The energies and populations are given for the occupied orbitals. The populations directly beneath the orbital are the total atomic charge in that orbital in units of electrons. (A) The populations in brackets under the I are the s and p populations in σ_2 and the s and d populations in σ_3. (B) The populations in brackets under the C and I are the s and p populations. The population in parentheses under the C is the population of the CF_3 group.

The electronic structure for **6** is significantly different from that of **8**. The HOMO and NHOMO for **6** are π orbitals at 6.27 and 6.52 eV and are the lone pairs on the iodines. The highest occupied σ orbital is the next orbital at 9.61 eV. A schematic of the σ orbitals is shown in Figure 7. The highest occupied σ orbital for **6** has the highest density at the central fluorine, 0.81e in the p_z orbital. The terminal fluorines have the next highest population, 0.34e in the p_z orbital. The iodine has the remaining density, 0.26e, predominantly in the s orbital with a population of 0.19e. The s orbital has negative overlap with both the p_z on F_c and the p_z on F_T. The small component of the d_z orbital on I behaves in the opposite way, bonding to both p_z on F_c and p_z on F. The next orbital is the second σ-bonding orbital at 11.89 eV. There is essentially a node at the central fluorine F_c and bonding interactions between I and F_T. The largest population is 0.66e in the p_z on F_T. There is 0.33e on the iodine divided between the s (0.18e) and p_z (0.15e) orbitals. The p_z orbitals are bonding whereas the s component on I is antibonding with respect to the p_z on F_T. The next three orbitals are the π lone pairs on the fluorines at 12.21 (F_c), 12.72 (F_T), and 12.75 (F_T) eV. The third occupied σ orbital is at 14.12 eV. This orbital is completely p_z in character, and there

Table VII. Calculated Structural Parameters for **7**

param	calc **7**	expt **4**[b]	expt **5**[b]
r(I–F_c)	2.347	2.482	2.452
r(C–I)	2.164	2.113	2.157
r(C–F)	1.386		1.355
θ(I–F_c–I)	180.0	169.0	155.8
θ(C–I–F_c)	180.0	176.2	178.6
θ(F-C–F)	104.7		106.3
θ(I–C–F)	113.9		110.2

[a] Bond distances in angstroms. Bond angles in degrees. [b] Averaged values from experiment where appropriate.

Table VIII. Fractional Coordinates (×10000) and Isotropic Thermal Parameters for **4**

atom	x	y	z	B_{iso}
I1	1591.4 (4)	1148.2 (3)	2946.1 (5)	2.1 (1)′
I2	−2368.4 (4)	1699.0 (3)	1721.5 (5)	2.0 (1)′
S1	9738 (1)	4195 (1)	2153 (2)	1.7 (1)′
F1	−324 (3)	1529 (3)	2256 (4)	3.3 (1)′
F12	3407 (4)	1428 (3)	5528 (4)	3.3 (1)′
F13	5589 (4)	1216 (3)	6187 (5)	4.5 (2)′
F14	6644 (4)	560 (3)	4546 (5)	4.2 (2)′
F15	5496 (4)	115 (3)	2235 (5)	4.0 (2)′
F16	3324 (4)	344 (2)	1551 (4)	3.2 (1)′
F22	−4159 (4)	2454 (2)	3074 (4)	3.2 (1)′
F23	−6368 (4)	2538 (3)	2435 (5)	3.5 (2)′
F24	−7477 (4)	1950 (3)	224 (5)	3.7 (1)′
F25	−6386 (4)	1198 (3)	−1249 (5)	3.7 (1)′
F26	−4176 (4)	1107 (2)	−626 (4)	3.3 (1)′
N1	9287 (5)	3897 (3)	3361 (6)	2.2 (2)′
N2	10019 (5)	3616 (3)	1169 (6)	2.2 (2)′
N3	11033 (5)	4412 (3)	2860 (6)	2.2 (2)′
C1	8091 (7)	3874 (4)	3160 (8)	2.9 (2)′
C2	9862 (7)	3329 (5)	4168 (7)	2.9 (2)′
C3	10832 (7)	3062 (4)	1506 (8)	2.6 (2)′
C4	9120 (6)	3470 (4)	84 (8)	2.7 (2)′
C5	11607 (7)	4728 (4)	1939 (9)	3.4 (3)′
C6	11105 (7)	4868 (4)	4004 (7)	2.8 (2)′
C11	3291 (6)	896 (4)	3512 (7)	2.0 (2)′
C12	3898 (7)	1106 (4)	4681 (8)	2.7 (2)′
C13	5009 (7)	1002 (4)	5030 (9)	2.8 (2)′
C14	5560 (7)	672 (4)	4189 (9)	3.0 (2)′
C15	4973 (6)	451 (4)	3045 (8)	2.7 (2)′
C16	3855 (6)	561 (4)	2682 (8)	2.3 (2)′
C21	−4086 (6)	1784 (4)	1240 (7)	1.8 (2)′
C22	−4677 (6)	2147 (4)	1985 (7)	1.9 (2)′
C23	−5816 (6)	2208 (4)	1666 (7)	2.3 (2)′
C24	−6385 (6)	1892 (4)	563 (8)	2.5 (2)′
C25	−5828 (6)	1527 (4)	−199 (8)	2.6 (2)′
C26	−4701 (6)	1476 (4)	135 (8)	2.3 (2)′
H1	7863	3685	3899	3.0
H1′	7790	3578	2447	3.0
H1″	7784	4322	2999	3.0
H2	9491	3216	4842	3.0
H2′	10602	3463	4555	3.0
H2″	9896	2920	3674	3.0
H3	10847	2787	762	3.0
H3′	10652	2778	2147	3.0
H3″	11539	3263	1794	3.0
H4	9343	3124	−454	3.0
H4′	8930	3881	−407	3.0
H4″	8495	3305	373	3.0
H5	12348	4849	2368	3.0
H5′	11249	5138	1583	3.0
H5″	11657	4409	1274	3.0
H6	11851	4978	4357	3.0
H6′	10785	4652	4633	3.0
H6″	10717	5298	3754	3.0

are no nodes between atoms. As would be expected, the largest population is on F_c (0.83e), and the next highest is on F_T (0.39e). There is only 0.20e in the p_z on the iodines. From the above results, one would expect the negative charge to be localized on the fluorines, and indeed the population on F_c is −0.60e and on F_T is −0.59e. The iodine is positive with a charge of +0.39e. The unoccupied σ orbitals are as expected, with the LUMO having

Table IX. Anisotropic Thermal Parameters (Å × 1000) $\exp[-19.739(U_{11}hha^*a^*... + 2(U_{12}hka^*b^*...))]$ for **4**

atom	U_{11}	U_{22}	U_{33}	U_{12}	U_{13}	U_{23}
I1	25.1 (2)	27.1 (3)	28.5 (3)	−0.7 (2)	5.4 (2)	2.2 (2)
I2	25.5 (3)	26.0 (3)	24.5 (3)	1.7 (2)	4.3 (2)	0.2 (2)
S1	28 (1)	18 (1)	21 (1)	2 (1)	6 (1)	1 (1)
F1	23 (2)	61 (3)	38 (3)	4 (2)	4 (2)	3 (2)
F12	42 (3)	48 (3)	36 (3)	3 (2)	5 (2)	−9 (2)
F13	55 (3)	55 (4)	50 (3)	−5 (3)	−11 (3)	−5 (3)
F14	22 (3)	53 (3)	81 (4)	5 (2)	4 (3)	17 (3)
F15	41 (3)	45 (3)	73 (4)	9 (2)	28 (3)	−5 (3)
F16	42 (3)	38 (3)	41 (3)	−1 (2)	7 (2)	−11 (2)
F22	49 (3)	45 (3)	28 (3)	4 (2)	7 (2)	−12 (2)
F23	44 (3)	49 (3)	50 (3)	9 (2)	27 (3)	−6 (2)
F24	27 (3)	55 (3)	56 (3)	4 (2)	4 (2)	2 (3)
F25	40 (3)	50 (3)	44 (3)	−7 (2)	−6 (2)	−13 (2)
F26	41 (3)	43 (3)	40 (3)	3 (2)	8 (2)	−19 (2)
N1	30 (3)	31 (4)	24 (3)	−3 (3)	9 (3)	4 (3)
N2	34 (4)	23 (3)	25 (3)	7 (3)	3 (3)	−1 (3)
N3	36 (4)	22 (3)	28 (4)	−7 (3)	10 (3)	3 (3)
C1	34 (4)	38 (5)	42 (5)	1 (4)	14 (4)	−3 (4)
C2	43 (5)	40 (5)	28 (4)	−2 (4)	6 (4)	17 (4)
C3	37 (5)	24 (4)	38 (5)	8 (3)	8 (4)	−3 (3)
C4	32 (4)	37 (5)	32 (5)	−2 (4)	4 (4)	−6 (4)
C5	43 (5)	37 (5)	51 (6)	−13 (4)	17 (4)	1 (4)
C6	45 (5)	35 (5)	27 (4)	−11 (4)	10 (4)	−10 (4)
C11	22 (4)	17 (4)	35 (4)	−2 (3)	1 (3)	3 (3)
C12	38 (4)	18 (4)	46 (5)	5 (3)	8 (4)	2 (4)
C13	36 (4)	21 (4)	43 (5)	1 (3)	−8 (4)	10 (4)
C14	29 (4)	29 (5)	54 (6)	−2 (4)	1 (4)	14 (4)
C15	29 (4)	24 (4)	50 (6)	3 (3)	12 (4)	8 (4)
C16	35 (5)	16 (4)	38 (5)	−4 (3)	8 (4)	4 (3)
C21	22 (4)	19 (4)	24 (4)	0 (3)	1 (3)	−1 (3)
C22	30 (4)	18 (4)	22 (4)	3 (3)	0 (3)	1 (3)
C23	32 (4)	23 (4)	34 (5)	3 (3)	12 (4)	2 (3)
C24	23 (4)	24 (4)	52 (5)	1 (3)	14 (4)	3 (4)
C25	29 (4)	29 (5)	37 (5)	−2 (3)	−2 (4)	1 (4)
C26	34 (5)	17 (4)	38 (5)	1 (3)	12 (4)	−5 (3)

Table X. Fractional Coordinates (×10000) and Isotropic Thermal Parameters for **5**

atom	x	y	z	B_{iso}
I1	3071.4 (1)	2500.0	7967.7 (4)	2.0 (1)′
I2	1137.4 (1)	2500.0	8211.9 (4)	2.1 (1)′
S1	3504 (1)	2500	3572 (1)	1.8 (1)′
F1	4050 (1)	1415 (4)	9178 (3)	5.1 (1)′
F2	4179 (1)	1405 (3)	6441 (2)	2.8 (1)′
F3	5031 (1)	1410 (3)	8197 (2)	3.0 (1)′
F4	5180 (1)	1411 (3)	5470 (3)	4.1 (1)′
F12	2100 (1)	2500	7575 (5)	3.3 (1)′
O40	1814 (2)	2500	3195 (5)	5.0 (2)′
N1	3969 (2)	2500	2343 (5)	2.0 (1)′
N2	3198 (1)	1112 (4)	3211 (3)	2.1 (1)′
C1	3921 (3)	2500	8422 (6)	2.7 (2)′
C2	4295 (2)	2500	7169 (6)	2.1 (1)′
C3	4915 (2)	2500	7454 (6)	1.9 (1)′
C4	5294 (2)	2500	6229 (6)	2.4 (2)′
C10	4307 (2)	1285 (5)	2368 (5)	2.9 (1)′
C21	2899 (2)	496 (5)	4331 (4)	2.5 (1)′
C22	2983 (2)	812 (5)	1863 (4)	2.4 (1)′
C41	1478 (5)	2500	2214 (11)	16.1 (11)′
C42	923 (4)	2500	2565 (13)	8.9 (5)′
C43	944 (5)	2500	4017 (12)	9.4 (5)′
C44	1493 (4)	2500	4303 (11)	14.8 (9)′
H10	4564	1323	1657	3.5
H10′	4085	514	2251	3.5
H10″	4491	1227	3201	3.5
H21	2733	−314	4025	3.5
H21′	2626	1097	4625	3.5
H21″	3138	300	5043	3.5
H22	2820	−53	1862	3.5
H22′	3268	827	1224	3.5
H22″	2719	1464	1628	3.5
H41	1546	3249	1606	10.0
H42	755	1701	2238	10.0
H43	779	1687	4314	10.0
H44	1551	1799	4826	10.0

Table XI. Anisotropic Thermal Parameters (Å × 1000) exp[−19.739($U_{11}hha^*a^*$... + 2($U_{12}hka^*b^*$...))] for **5**

atom	U_{11}	U_{22}	U_{33}	U_{12}	U_{13}	U_{23}
I1	24.5 (2)	29.9 (2)	20.8 (2)	0.0	1.2 (1)	0.0
I2	24.8 (2)	22.8 (2)	33.1 (2)	0.0	−3.0 (1)	0.0
S1	34 (1)	19 (1)	17 (1)	0	−4 (1)	0
F1	39 (1)	112 (3)	44 (2)	16 (2)	4 (1)	47 (2)
F2	34 (1)	37 (2)	36 (1)	−4 (1)	−2 (1)	−11 (1)
F3	32 (1)	41 (2)	41 (1)	6 (1)	−1 (1)	17 (1)
F4	39 (1)	71 (2)	44 (2)	−9 (1)	3 (1)	−33 (2)
F12	29 (2)	36 (2)	60 (2)	0	−3 (2)	0
O40	53 (3)	97 (5)	41 (3)	0	6 (2)	0
N1	31 (2)	21 (3)	23 (2)	0	2 (2)	0
N2	40 (2)	25 (2)	14 (1)	−7 (2)	0 (1)	−1 (1)
C1	40 (3)	52 (4)	13 (3)	0	−1 (2)	0
C2	26 (3)	31 (3)	21 (3)	0	−3 (2)	0
C3	25 (3)	23 (3)	26 (3)	0	−4 (2)	0
C4	25 (3)	41 (4)	25 (3)	0	−2 (2)	0
C10	42 (2)	25 (3)	44 (3)	8 (2)	1 (2)	1 (2)
C21	42 (2)	29 (2)	25 (2)	−5 (2)	6 (2)	2 (2)
C22	37 (2)	33 (2)	20 (2)	−7 (2)	−5 (2)	−7 (2)
C41	57 (6)	504 (40)	51 (7)	0	−3 (5)	0
C42	59 (6)	195 (17)	82 (8)	0	−15 (6)	0
C43	68 (7)	225 (18)	65 (7)	0	17 (5)	0
C44	52 (6)	457 (33)	52 (6)	0	4 (5)	0

three nodes, one at the F_c (there is some s character) and nodes between F_T and I. The final unoccupied σ orbital has four nodes, one between each atom.

The optimized geometry for **7** is given in Table VII. Due to the number of basis functions, force constants were not obtained, but on the basis of the results found for **6** and **8**, we expect a D_{3h} structure. The calculated I–F_c bond length in **7** is 0.10 Å less than the observed value in **5** and 0.13 Å less than the observed value in **4**. However, the calculated I–F_c bond in **7** is 0.07 Å longer than the value in **6**, suggesting that the interaction of the R_f–I fragments in **7** with the F^- is weaker than the interaction of the I–F fragments with F^- in **6**. This is consistent with F being better able to stabilize the terminal position (excess negative charge) of the 5c 6e bond than does a CF_3 group. The n-C_4F_8I fragment is not as good a stabilizing group as CF_3 and consequently the I–F_c bonds are longer in **5**. A similar result is expected for **4**, with the pentafluorophenyl fragment being even less able to stabilize the terminal position in the 5c 6e bond. As would be expected, the values of r(C–I) decrease as I–F_c increases. The value for r(C–I) in **7** is only 0.03 Å longer than the calculated value for CF_3I. The C–I bonds in **5** are similarly elongated. The C–I bonds in **4** show little elongation, consistent with a smaller interaction, although the I is bonded to an sp^2 carbon, making the comparison difficult. The C–F bond lengths in **7** are 0.02 Å longer than those in CF_3I. The bond angle θ(F–C–F) is 2.3° smaller in **7** than the value calculated for CF_3I. These results are essentially the same as those found when the two different CF_2 groups in **5** are compared. The changes in C–F bond length and in θ(F–C–F) are indicative[2,29] of carbanionic character at the carbon bonded to iodine. However, the changes at the CF_3 groups in **7** as compared to those in CF_3I are not as pronounced as the changes found in **8** when compared to CF_3I. This is consistent with the CF_3 group in **7** stabilizing less negative charge than the CF_3 group in **8**.

Besides the differences in I–F bond lengths between **7** and **4** and **5**, there are also differences in angles. The angles centered at iodine θ(C–I–F_c) in **4** and **5** deviate less than 4° from 180°. This is similar to the deviation found in $[C_6F_5$–I–$C_6F_5]^-$ as compared to **8**; **4** and **5** are quasi-linear at iodine. The deviations from linearity at F_c are more substantial, 11° for **4** and 24.2° for **5**. However, these deviations could well be due to crystal-packing forces. The lowest energy bending mode in **6** has a large component of motion involving F_c and is only 28 cm^{-1}, 0.08 kcal/mol. In **4** and **5**, the R_f–I interactions with F_c are even weaker than the F_c–I interactions found in **6** (r(I–F_c) is almost 0.20 Å longer in **4** and **5**). Thus, the bending frequency should decrease and crystal-packing forces could easily cause the observed deviations from linearity at F_c.

The charge distributions for **7** are consistent with the above structural comparisons. The charge on F_c is −0.69e, a change of −0.09e as compared to the charge in **6**. The terminal CF_3 groups are negative, but the charge is only −0.39e (divided as −0.33e on F and +0.60e on C) as compared to the charge on F_T of −0.59e in **6**. The iodines in **7** have a significantly reduced positive charge, +0.22e as compared to +0.39e in **6**.

The σ-bonding orbitals in **7** show the expected changes (Figure 7). As found for **6**, the HOMO (7.25 eV) and NHOMO (7.49 eV) are π orbitals composed of the lone pairs on the iodines. The highest occupied σ orbital is at 8.61 eV and has essentially the same shape as the orbital found in **6**. The p_z component on F_c is lower in **7** with only 0.68e. The population on the iodines is essentially unchanged at 0.28e, and the charge on the CF_3 groups is increased to +0.38e. (There is 0.28e on the carbon, 0.18e in p_z, and 0.10e in s.) In the next σ orbital (10.57 eV), there is a node at the central fluorine. There is 0.41e on the iodine (0.29e p_z and 0.12e s) and 0.59e on the CF_3 groups. Of this 0.59e, only 0.34e is on the carbon, 0.23e in the p_z, and 0.11e in the s. The fluorine lone-pair π orbital on the central atom is at 11.60 eV followed by the lowest lying σ orbital. As would be expected, the population on the central fluorine has increased to 0.97e as compared to 0.83e in **6**. The iodines have a population of 0.21e and the CF_3 groups each have 0.30e. The population on the CF_3 groups in this orbital is distributed over all of the atoms with only 0.09e on the carbons. Thus, as the I–F_c bond lengthens, the central fluorine has more anionic character. However, even in **7**, there is still a large σ-bonding component, and a 5c 6e bond is present. The σ^* orbitals have the appropriate form, essentially three nodes in the LUMO and four nodes in the NLUMO.

Discussion

The occurrence of bridging fluoride ions is a common theme for a wide variety of structures.[31] For example, near-linear fluoride bridges have been structurally characterized in Te, Yb, and Sn complexes. Other workers have described weak interactions between F and I in $[ICl]^+[SbF_5]^-$,[32a] the complex between IF·pyr and IF_5·pyr[32b] and in XeF_2·IF_5.[32c] However, none of these examples deal with similar ensembles of atoms (with respect to connectivities or formal oxidation state), so direct comparison of I–F distances is of limited value. None of the above examples have F^- binding two neutral molecules with "normal" valency at the atom bonding to the fluorine. There is one structure[33] to which we can compare that is formally isoelectronic to **6**; that is $Xe_2F_3^+$, where an "F^-" bridges two XeF^+ cations. The ion $Xe_2F_3^+$ (Table VI) has a linear arrangement at Xe whereas, at F_c, the bond angle deviates 30° from linearity. Both the Xe–F_c and Xe–F_T bond distances in $Xe_2F_3^+$ are shorter than the corresponding I–F bond distances in **6**, consistent with the result that the Xe is formally positive whereas the I is neutral. Whether the deviation from

(31) (a) Alcock, N. W. In *Advances in Inorganic Chemistry and Radiochemistry*; Emeleus, H. J., Sharpe, A. G., Eds.; Academic: New York, 1972; Vol. 15, p 1. (b) $Mo_4(\mu$-F)$_4$(O-*t*-Bu)$_8$: Chisholm, M. H.; Clark, D. L.; Hoffman, J. C. *Polyhedron* **1985**, *4*, 1203. (c) $(UF_2O_2{\cdot}3S_bF_5)$: Fawcett, J.; Holloway, J. H.; Laycock, D.; Russell, D. R. *J. Chem. Soc., Dalton Trans.* **1982**, 1355. (d) $[((PMePh_2)_3H_2Mo)_2(\mu$-F)$_3]^+$: Crabtree, R. H.; Hlatky, G. G.; Holt, E. M. *J. Am. Chem. Soc.* **1983**, *105*, 7302. (e) {Ucp″$_2$ (μ-BF_4)(μ-F)}$_2$ (cp″ = $C_3H_3(SiMe_3)_2$): Hitchcock, P. B.; Lappert, M. F.; Taylor, R. G. *J. Chem. Soc., Chem. Commun.* **1984**, 1082. (f) $[(\eta$-$C_5H_5)_2ScF]_3$: Bottomley, F.; Paez, D. E.; White, P. S. *J. Organomet. Chem.* **1985**, *291*, 35. (g) $[(Me_2N)_2TiF_2]_4$: Sheldrick, W. S. *J. Fluorine Chem.* **1974**, *4*, 415. (h) $[MoO(O_2)(pydca)]_2F^-$: Edwards, A. J.; Slim, D. R.; Guerchais, J. E.; Kergoat, R. *J. Chem. Soc., Dalton Trans.* **1980**, 289. (i) [MeN=WF_4—F—WF_4=NMe]$^-$: Chambers, O. R.; Harman, M. E.; Rycroft, D. S.; Sharp, D. W. A. *J. Chem. Res., Miniprint* **1977**, 1846. (j) KF·2Al$(C_2H_5)_3$: Ziegler, K.; Koster, R.; Lehmkuhl, H.; Reinert, K. *Liebigs Ann. Chem.* **1960**, *629*, 33. Allegra, G.; Perego, G. *Acta Crystallogr.* **1963**, *16*, 185. (k) K[Al_2-$(CH_3)_6F]{\cdot}C_6H_6$: Atwood, J. L.; Newberry, W. R. *J. Organomet. Chem.* **1974**, *66*, 15. (l) $([TeF_3]^+[Sb_2F_{11}]^-)$: Edwards, A. J.; Taylor, P. *J. Chem. Soc., Dalton Trans.* **1973**, 2150. (m) $[(OC)_5ReFRe(CO)_5]^+$: Raab, K.; Beck, W. *Chem. Ber.* **1985**, *118*, 3830. (n) Katz, H. E. *J. Org. Chem.* **1985**, *50*, 5027.

(32) (a) $([ICl_2]^+[SbF_6]^-)$: Birchall, T.; Myers, R. D. *Inorg. Chem.* **1981**, *20*, 2207. (b) (IF·IF_5·2pyr): Lehmann, E.; Naumann, D.; Schmeisser, M. *J. Fluorine Chem.* **1976**, *7*, 135. (c) XeF_2·IF_5: Jones, G. R.; Burbank, R. D.; Bartlett, N. *Inorg. Chem.* **1970**, *9*, 2264.

(33) Sladky, F. O.; Bulliner, P. A.; Bartlett, N.; DeBoer, B. G.; Zalkin, A. *Chem. Commun.* **1968**, 1048.

linearity is due to crystal forces or to an inherent property of the ion requires further testing. The observed Raman spectrum[34] for $Xe_2F_3^+$ has bands assigned to the Xe–F_T stretches at 598 and 588 cm^{-1}, consistent with our calculated values of 578 and 573 cm^{-1} for the I–F_T stretches in **6**. The difference would be larger if we scaled our values by the ratio $\nu_{obs}/\nu_{calc} = 0.90$ found for IF in order to account for our neglect of correlation and anharmonic corrections. Our scaled values are 520 and 516 cm^{-1}. The $Xe_2F_3^+$ frequencies should be higher than our values due to the shorter Xe–F bond lengths due to the presence of a formally positive Xe. The symmetric and asymmetric Xe–F_c–Xe stretches are assigned as 417 and 401 cm^{-1}. This value seems high for the asymmetric stretch and is clearly too high for the symmetric stretch. Bending modes at 255 and 163 cm^{-1} are consistent with our calculated values for **6**. However, the very low bends that we predicted were not observed due to the width of the excitation line in the Raman spectrum. The available results on $Xe_2F_3^+$ are consistent with our model for $I_2F_3^-$ and suggest that the σ bonding in $Xe_2F_3^+$ is best described as a 5c 6e bond.

Our results clearly confirm the presence of a 5c 6e bond in **6** and **7** and by extension to **4** and **5** and the remaining observed species. The other possibility for these systems would be an ion–dipole system where the central fluorine is F^- binding two neutral R_f–I molecules. In this case the σ orbitals would have no density in σ_1 and σ_2 (Figure 1) on F_c and all of the density in σ_3 on F_c as shown here. This orbital scheme is clearly not found in our calculations.

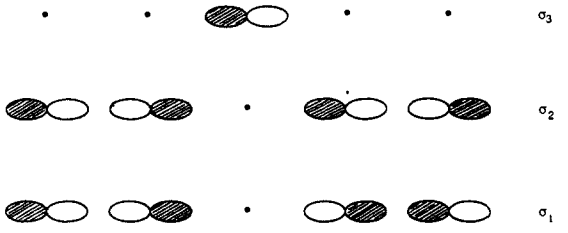

The 5c 6e bonding scheme differs in its electronic requirements as compared to the 3c 4e bonding scheme. The 3c 4e bonding scheme has a node at the central atom and all of the density on the terminal atoms in the HOMO. Thus, the 3c 4e bond prefers to have the atom with the lowest electronegativity in the center and the most electronegative groups at the terminal positions. This result is well-known and has been observed in a wide range of systems. The 5c 6e bond is significantly different in that the HOMO has nodes at atoms 2 and 4 and the highest density is on the central atom and on the terminal positions. As in the case of the 3c 4e bond, the terminal atoms should still be very electronegative. The central atom should also be very electronegative, exactly the opposite of what is observed for the 3c 4e bond. Positions 2 and 4 should now be the least electronegative elements. This simple analysis is consistent with the observed structures, electropositive iodines (or Xe) at 2 and 4, an electronegative fluorine in the central, and electronegative R_f's or F's at the terminal positions. For the anions under consideration here, the ability of the terminal group to stabilize excess negative charge is important in determining the strength of the interactions in the 5c 6e bond. As noted earlier, the I–F_c bond distance increases and the R_f–I bond distance decreases as the ability of the terminal group to stabilize negative charge decreases ($F > CF_3 > \sim CF_2{\cdot}CF_2 > C_6F_5$), consistent with this result. Even though the strength of the interactions in the 5c 6e bond are decreasing, these structures are still in the chemical-bonding continuum as opposed to the van der Waals bond continuum. The sum of the van der Waals radii for I interacting with F is 3.5–3.6 Å. The longest I–F bond distance that we observe is 2.51 Å in **4**, and it is 1 Å *shorter* than the van der Waals interaction, clearly still in the chemical-bonding regime.

Conclusions

The crystal structure analysis shows the presence of fluorine in a unique bonding environment. Our calculations allow us to define this environment as a 5c 6e σ bond with fluorine at the central position. The electronic requirements of the 5c 6e bond differ from those of the 3c 4e bond. In the 5c 6e bond, the central and terminal positions should be occupied by electronegative elements (or groups) whereas in the 3c 4e bond only the terminal positions are occupied by electronegative elements. The remaining two positions in the 5c 6e bond and the central position in the 3c 4e bond should be occupied by more electropositive atoms. These results allow us to extend the concept of the hypervalent σ bond.

Acknowledgment. We thank A. J. Arduengo, III, for many discussions on the definition of the hypervalent bond.

Registry No. 2 (TAS = $(Me_2N)_3S^+$), 100645-92-9; **3**, 1584-03-8; **4**, 117183-73-0; **5**, 117162-30-8; **6**, 117162-35-3; **9**, 117162-31-9; **10**, 117162-32-0; **11**, 117162-33-1; **12**, 117162-34-2; CF_3I, 2314-97-8; CF_3^-, 54128-17-5; F^-, 16984-48-8; pentafluorophenyl iodide, 827-15-6; 1,4-diiodooctafluorobutane, 375-50-8; perfluoro-*n*-hexyl iodide, 355-43-1; 1,2-diiodotetrafluoroethane, 354-65-4; 1,8-diiodohexadecafluorooctane, 335-70-6; 1,10-diiodoeicosafluorodecane, 65975-18-0; benzyl bromide, 100-39-0; benzyl fluoride, 350-50-5; *O*-(trimethylsilyl)phenol, 1529-17-5; 4-phenoxy-2,3,5,6-tetrafluoro-1-iodobenzene, 117162-36-4.

(34) Gillespie, R. J.; Landa, B. *Inorg. Chem.* **1973**, *12*, 1383.